

A light scalar particle from strong dynamics in a new holographic model of QCD

Mark Van Raamsdonk and Kevin Whyte

Department of Physics and Astronomy, University of British Columbia
6224 Agricultural Road, Vancouver, B.C., V6T 1W9, Canada

Abstract

We study a new holographic gauge theory based on an ND=2 intersecting D4-D4 system. The theory depends on a parameter $y_0 \in [y_*, \infty)$ which controls the asymptotic behavior of the probe D4-branes. For $y_0 = y_*$, the theory has massless mesons associated with a spontaneous global symmetry breaking $SU(2) \times SU(2) \rightarrow SU(2)$. For large y_0 , the meson masses behave as $m^2 \propto y_0$, except for a single light meson with $m^2 \propto 1/y_0^2$. The parametric lightness of this scalar particle is not directly related to any approximate symmetry of the field theory. Field theory configurations with baryons correspond to smooth embeddings of the probe D4-branes with nontrivial winding around an S^4 in the geometry. As a consequence, physics of baryons and nuclei can be studied reliably in this model using the abelian Born-Infeld action.

1 Introduction

Gauge-theory / gravity duality [1] provides a powerful tool to construct and study strongly coupled field theory systems. In recent years, the set of field theories constructed and analyzed in this way has grown to include examples which are qualitatively similar to systems of great physical interest, including QCD (see e.g. [2, 3, 4, 5, 6, 7]), superconductors, superfluids, quantum hall systems, and cold atom systems (see [8, 9] for recent reviews of applications to condensed matter systems). While it may be too optimistic to expect that we will be able to find gravitational systems that are exactly dual to real QCD or specific real-world condensed matter systems, these model systems can provide significant qualitative insight into generic phenomena that arise in strongly coupled systems similar to the real-world examples. There are already examples (e.g. the very low viscosity to entropy ratio for the quark-gluon plasma produced in heavy ion collisions) where the insight gained from holographic models offers the best theoretical understanding of an experimentally measured phenomenon (see e.g. [10, 11, 12]).

With such potential for new theoretical insight into physically interesting systems, it seems fruitful to explore a wide variety of holographically constructed field theories. In doing so, we may uncover new qualitative phenomena in strongly coupled field theories that could help explain real-world physical phenomena or, more generally, lead to an improved understanding of quantum field theory at strong coupling. In addition, amassing a large number of detailed examples will help reveal which features of these systems are generic (and thus more likely to apply to other systems for which we may not have a precise gravity dual), and which are peculiar to specific constructions.

Motivated by these considerations, we study in this paper a new holographic field theory closely related to the Sakai-Sugimoto model [7] of holographic QCD. Specifically, our theory has the same adjoint sector, but a different fundamental sector since we use probe D4-branes instead of probe D8-branes. Thus, our model is based on a brane construction where both the “color branes” (which give rise to the adjoint sector) and the “flavor branes” are D4-branes. The relative orientation for the two sets of branes is:

	0	1	2	3	4	5	6	7	8	9
N_c D4	×	×	×	×	×					
N_f D4	×	×	×	×		×				

as shown in figure 1. At weak coupling, this system has a (complex scalar) tachyon in its low-energy spectrum coming from the D4-D4' strings. However, by separating the branes in a transverse direction (e.g. the 6 direction), we can arrange for this tachyon to become massless or massive. The lightest D4-D4' fermions have string scale masses in this case. For the original theory with no transverse separation, the geometrical $SO(5)$ symmetry present in the adjoint sector of the theory is broken to $SO(4)$, while the theory defined with a transverse separation between the two sets of branes has this symmetry broken to $SO(3)$.

In order to obtain a decoupled field theory, we want to take a low-energy decoupling

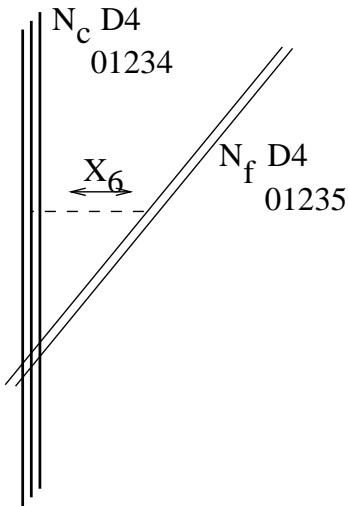


Figure 1: Brane construction for the holographic field theory.

limit in this brane setup. We would like to do this in such a way that the lightest modes of the D4-D4' strings survive. It is plausible that we can tune the transverse separation of the two sets of branes as we take the limit to achieve this. In practice, we do not actually define an explicit decoupling limit starting from a brane configuration in asymptotically flat space. Instead, we do something much simpler (following the Sakai-Sugimoto example). We will always consider the limit where $N_f \ll N_c$, so that the fundamental matter does not affect the physics of the adjoint sector (i.e. the quenched approximation is accurate). Then the addition of fundamental matter can be achieved simply by adding probe D4-branes into the geometry dual to the field theory describing the low-energy degrees of freedom of the N_c D4-branes. Thus, instead of starting with color and flavor branes in asymptotically flat space, we just look for a stable configuration of probe D4-branes in the geometry dual to the color branes such that the configuration preserves the desired symmetries.

Since we are working in a consistent background of string theory, we can say that the model we describe is some fully consistent quantum field theory sharing many qualitative features with QCD. Based on the weak coupling picture, it is tempting to suggest that the model we describe is one where the fundamental quarks are purely scalar, since the D4-D4' fundamental fermions have string scale masses when the branes are tuned to make the lightest scalar massless or massive. Achieving a model with scalar quarks was one of the original motivations for studying this model, since we were interested to look at the qualitative similarities and differences between our model and the Sakai-Sugimoto model (where the fundamental matter is fermionic), and also to see whether any new qualitative phenomena appear in the physics of strongly coupled fundamental bosons. However, since our actual construction is less direct than an explicit decoupling limit, we cannot say definitively that the model includes only scalar quarks.

Outline and Summary

After a review of the basic setup in section 2, we carry out the analysis of probe brane embeddings in section 3, focusing on the case $N_f = 1$. We find a one-parameter family of locally-stable D4-brane embeddings.¹ These are labeled by a parameter $y_0 \in [y_*, \infty)$ that measures how far into the IR of the geometry the probe brane reaches ($y = 1$ corresponds to the IR end of the geometry, while $y_* = 1.09038..$ is the minimum value for a stable embedding). The embeddings in this family correspond to the vacuum solutions for a one-parameter family of field theories. In each case, the solution preserves $SO(3) \sim SU(2)$ global symmetry, but for $y = y_*$, this symmetry arises via a spontaneous breaking from $SO(4) \sim SU(2) \times SU(2)$. For this special case, there is a family of solutions with the same $SO(4)$ -preserving asymptotics. Each of the solutions preserves only $SO(3)$, and we have an $SO(3)$ vector of massless scalar goldstone bosons associated with the broken symmetry. These mesons get a mass as we increase y_0 , and for all larger values of y_0 , all the mesons (which correspond to small fluctuations about the original brane configuration) are massive. For all but one of the meson states, we find that the mass behaves like $m^2 \propto y_0$ for large y_0 , consistent with an interpretation of y_0 as the mass-squared of the fundamental scalar quarks in the model. However, there is a single scalar particle (an $SO(3)$ singlet) whose mass *decreases* for large y_0 as $m^2 \propto 1/y_0^2$. Thus, for large y_0 we have a single scalar particle that is parametrically lighter than all the other mesons. This lightness is not a consequence of any approximate symmetry, but is related to the “generalized conformal symmetry” of the near-horizon D4-brane background, which involves a scaling of the radial coordinate together with a transformation of the string coupling. In the limit $y_0 \rightarrow \infty$ where the mass goes to zero, the meson sector completely decouples from the theory. A detailed discussion of this light scalar may be found in section 4, which begins with our presentation of the complete fluctuation analysis to determine the bosonic meson spectrum. Our results for the spectrum are summarized in figure 2.

Perhaps the most interesting feature of our model that the baryonic sector can be studied very reliably, as we discuss in section 5. As in the Sakai-Sugimoto model, baryon charge arises from D4-branes which wrap an S^4 in the geometry (see section 5 for a review). But in our D4-D4 system, these wrapped D4-branes can smoothly reconnect with the probe D4-branes of the original embedding. Thus, states in the field theory with nonzero baryon number correspond to smooth D4-brane embeddings of different topology from the vacuum embedding. Baryon charge in the field theory corresponds in the bulk to a topological charge $\pi_4(S^4)$ for the embedding (relative to the original embedding). These smooth embeddings can be studied reliably using the abelian Born-Infeld action, so properties such as baryon mass and nuclear binding energies should be under complete control in the model. This is in contrast to the

¹A holographic field theory corresponding to a different class of probe D4-brane embeddings was studied in [13] among other examples. In that case, the nontrivial directions for the D4-brane embedding were the compact field theory direction x_4 and the radial direction (as in Sakai-Sugimoto) while in our case, the embedding corresponds to a nontrivial path in the radial direction and the S^5 surrounding the color D4-branes, as in figure 1. Another model with D4-brane probes in a different background was studied in [14].

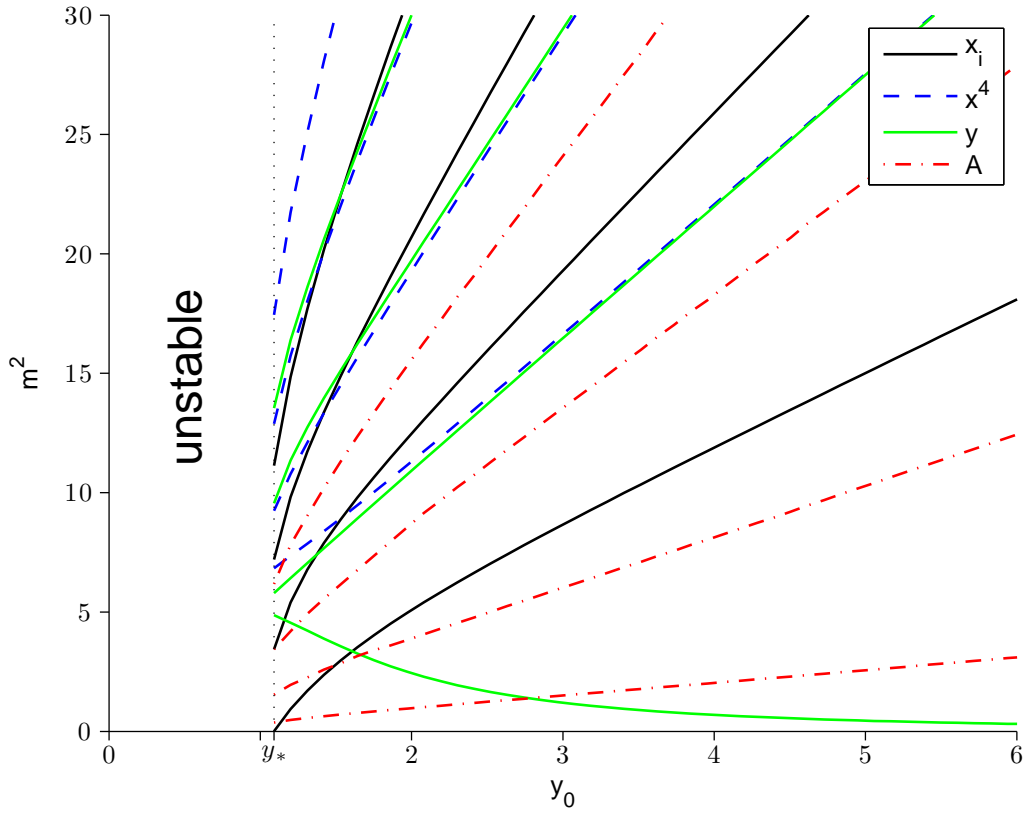


Figure 2: Spectrum of low-lying bosonic mesons as a function of the embedding parameter y_0 . For $y_0 = y_*$, we have massless goldstone bosons associated with $SU(2) \times SU(2) \rightarrow SU(2)$ symmetry breaking. For large y_0 , a single scalar meson becomes parametrically light.

Sakai-Sugimoto model, where baryons are described by instanton-like configurations of the Yang-Mills fields on the probe D8-branes whose size is string-scale. In that case, higher α' corrections to the Born-Infeld action should be important for a completely reliable treatment of baryon physics.²

In section 6, we study the theory at finite temperature. We recall that above a critical temperature, the theory is in a deconfined phase [2, 17], manifested in the bulk picture by a black brane geometry. In similar holographic field theories, probe brane embeddings in a deconfined phase either sit completely outside the black hole (the “Minkowski embeddings” where we still have non-dissociated mesons) or extend all the way to the horizon (the “black hole embeddings” where all mesons are dissociated) [5]. In our case, the theories that admit stable embeddings at low temperature have only black hole embeddings at high temperature, so all mesons “melt” at the deconfinement transition.

More discussion of the baryon sector of the model, as well as a study of this model at finite baryon density, will appear in a follow-up paper [20].

2 Setup

In this section, we review the basic construction of our holographic field theory. We begin by describing the adjoint sector, and then describe the addition of flavor fields via the embedding of probe branes in the dual geometry.

2.1 Adjoint sector

The adjoint sector of our model was originally proposed by Witten [2] as a construction of non-supersymmetric Yang-Mills theory. It is defined by the low-energy decoupling limit of N_c D4-branes wrapped on a circle of length $2\pi R$ with anti-periodic boundary conditions for the fermions. This part of the theory has two dimensionless parameters, N_c and a coupling constant

$$\lambda = \frac{\lambda_{D4}}{2\pi R},$$

where

$$\lambda_{D4} = g_{YM}^2 N_c.$$

The dimensionless parameter λ is the effective four-dimensional coupling at the Kaluza-Klein scale. For small λ , this coupling runs to strong coupling at a smaller scale

$$\Lambda_{QCD} \sim \frac{1}{R} e^{\frac{-c}{\lambda}}$$

where the physics should be exactly that of pure 3+1 dimensional Yang-Mills theory (thanks to fermion masses generated by the antiperiodic boundary conditions and scalar

²There have nevertheless been many studies of baryons and baryon physics in the Sakai-Sugimoto model making use of various approximations, see e.g. [16] for some of the early work.

masses generated at one loop). For large λ , the dual gravity theory becomes weakly curved, and physics is well described by type IIA supergravity on a background

$$\begin{aligned} ds^2 &= \left(\frac{U}{R_4}\right)^{\frac{3}{2}} (\eta_{\mu\nu} dx^\mu dx^\nu + f(U) dx_4^2) + \left(\frac{R_4}{U}\right)^{\frac{3}{2}} \left(\frac{1}{f(U)} dU^2 + U^2 d\Omega_4^2\right) \\ e^\phi &= g_s \left(\frac{U}{R_4}\right)^{\frac{3}{4}} \\ F_4 &= \frac{2\pi N_c}{\omega_4} \epsilon_4. \end{aligned} \tag{1}$$

Here ω_4 is the volume of a unit 4-sphere, ϵ_4 is the volume form on S^4 , and

$$f(U) = 1 - \left(\frac{U_0}{U}\right)^3. \tag{2}$$

The x_4 direction, corresponding to the Kaluza-Klein direction in the field theory, is taken to be periodic, with coordinate periodicity $2\pi R$, however, it is important to note that this x_4 circle is contractible in the bulk since the x_4 and U directions form a cigar-type geometry.

The parameters R_4 and U_0 appearing in the supergravity solution are related to the string theory parameters by

$$R_4^3 = \pi g_s N_c l_s^3 \quad U_0 = \frac{4\pi}{9R^2} g_s N_c l_s^3$$

while the four-dimensional gauge coupling λ is related to the string theory parameters as

$$\lambda = 2\pi \frac{g_s N_c l_s}{R}.$$

In terms of the field theory parameters, the dilaton and string-frame curvature at the tip of the cigar (the IR part of the geometry) are of order $\lambda^{\frac{3}{2}}/N_c$ and $\sqrt{\lambda}$, so as usual, supergravity will be a reliable tool for studying the infrared physics when both λ and N_c are large (in this case, with $N_c \gg \lambda^{\frac{3}{2}}$).

2.2 Fundamental matter

The addition of fundamental matter manifests itself through the appearance of N_f probe D4-branes in the geometry dual to the adjoint sector. These D4-branes are extended along the x^μ directions, sit at a point in the x^4 direction, and are described by a one-dimensional path in the remaining radial and sphere directions. It is convenient to redefine coordinates so that the metric in these directions takes the form

$$\alpha(\rho)(d\rho^2 + \rho^2 d\Omega_4^2) \tag{3}$$

These coordinates should satisfy

$$\frac{dU}{U\sqrt{f(U)}} = \frac{d\rho}{\rho}$$

From this, we find the map

$$\frac{U}{U_0} = \left(\frac{1}{2} \left(\frac{\rho}{\rho_0} \right)^{\frac{3}{2}} + \frac{1}{2} \left(\frac{\rho_0}{\rho} \right)^{\frac{3}{2}} \right)^{\frac{2}{3}} .$$

where $\rho_0 = U_0 2^{-\frac{2}{3}}$. Locally, the metric (3) is conformally equivalent to R^5 , however we should note that the space has an infrared end at $\rho = \rho_0$ where the X^4 circle contracts to a point. Thus, the ball $\rho < \rho_0$ is not part of the geometry.

We expect that the stable configurations will lie in a single plane in the R^5 appearing in (3), so it will sometimes be convenient to use coordinates

$$d\rho^2 + \rho^2 d\Omega_4^2 = dr^2 + r^2 d\theta^2 + d\vec{x}_T^2$$

in terms of which the equilibrium D4-brane configurations will be specified by $\vec{x}_T = 0$ and $r(\theta) = \rho(\theta)$ (note that $\rho = r$ for $\vec{x}_T = 0$).

To write the action for the probe D4-branes, we focus on the case of a single brane, for which we can use the abelian Born-Infeld action

$$S = -\mu_4 \int d^5\sigma e^{-\phi} \sqrt{-\det(g_{ab} + \tilde{F}_{ab})} \quad (4)$$

where

$$\tilde{F} = 2\pi\alpha' F .$$

We choose static gauge $X^\mu = \sigma^\mu$ for the field theory directions, and describe the nontrivial part of the embedding by functions $X^4(\sigma), r(\sigma), \theta(\sigma), X_T^i(\sigma)$, where σ parameterizes the remaining coordinate along the brane. The pull-back metric appearing in the Born-Infeld action is then given explicitly by

$$\begin{aligned} g_{\mu\nu} &= G_{\mu\nu} + G_{44}\partial_\mu X_4\partial_\nu X_4 + G_{rr}\partial_\mu r\partial_\nu r + G_{\theta\theta}\partial_\mu\theta\partial_\nu\theta + G_{ij}\partial_\mu X_T^i\partial_\nu X_T^j \\ g_{\mu\sigma} &= G_{44}\partial_\mu X_4\partial_\sigma X_4 + G_{rr}\partial_\mu r\partial_\sigma r + G_{\theta\theta}\partial_\mu\theta\partial_\sigma\theta + G_{ij}\partial_\mu X_T^i\partial_\sigma X_T^j \\ g_{\sigma\sigma} &= G_{44}\partial_\sigma X_4\partial_\sigma X_4 + G_{rr}\partial_\sigma r\partial_\sigma r + G_{\theta\theta}\partial_\sigma\theta\partial_\sigma\theta + G_{ij}\partial_\sigma X_T^i\partial_\sigma X_T^j \end{aligned}$$

For now, we are interested in equilibrium brane configurations, which we assume have $X^4 = X_T^i = 0$, so we keep only terms in the action involving $r(\sigma)$ and $\theta(\sigma)$. With this simplification, the action becomes

$$S = -\mu_q \int d\sigma H(r(\sigma)) \sqrt{r^2 \left(\frac{d\theta}{d\sigma} \right)^2 + \left(\frac{dr}{d\sigma} \right)^2} \quad (5)$$

where

$$H(r) = \frac{r^{\frac{3}{2}}}{R^{\frac{3}{2}}} \left(1 + \frac{\rho_0^3}{r^3} \right)^{\frac{5}{3}}$$

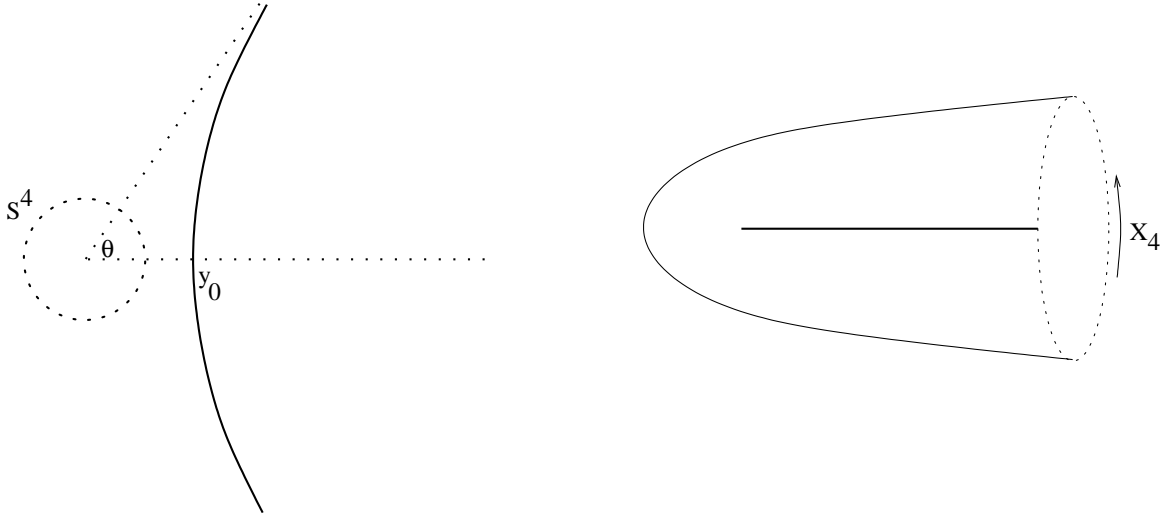


Figure 3: Schematic of a brane embedding. Left picture shows a plane in the space formed by the radial direction and the S^4 directions. Right picture shows same embedding in radial and x_4 directions.

3 Vacuum solutions

For our calculations of the vacuum configurations, it is convenient to fix the remaining reparametrization invariance by choosing $\sigma = \theta$. If we also define

$$y = \frac{r}{\rho_0} ,$$

the resulting action is

$$S = -\mu_4 \rho_0 \left(\frac{\rho_0}{R_3} \right)^{\frac{3}{2}} \int d\theta h(y) \sqrt{y^2 + (y')^2}$$

where

$$h(y) = y^{\frac{3}{2}} \left(1 + \frac{1}{y^3} \right)^{\frac{5}{3}} .$$

Since the resulting action does not depend on θ , we have a θ -independent quantity

$$y' \frac{\partial S}{\partial y'} - S = \frac{h(y)y^2}{\sqrt{y^2 + (y')^2}}$$

The brane configurations that we find all have some minimal value of y for which $y' = 0$. Calling this value y_0 , we have

$$\frac{h(y)y^2}{\sqrt{y^2 + (y')^2}} = h(y_0)y_0$$

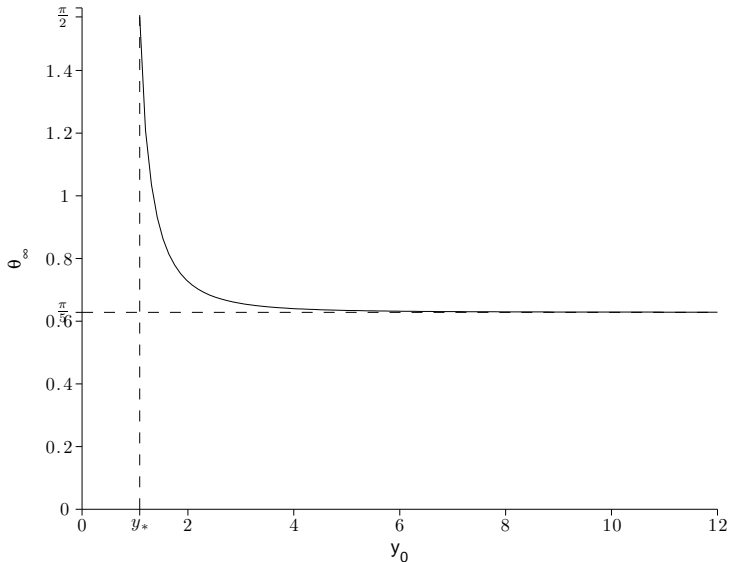


Figure 4: Asymptotic angle on S^4 vs minimum radial position for probe D4-brane embeddings. Function asymptotes to infinity at $y_0 = 1$. Values of θ_∞ in $(\pi/5, \pi/2]$ correspond to stable embeddings.

which gives

$$\frac{dy}{d\theta} = \pm y \sqrt{\frac{h^2(y)y^2}{h^2(y_0)y_0^2} - 1}.$$

Integrating, we find

$$\theta(y) = \int_{y_0}^y dx \frac{1}{x \sqrt{\frac{y_0^5(1+x^3)^{\frac{10}{3}}}{x^5(1+y_0^3)^{\frac{10}{3}}} - 1}}. \quad (6)$$

where we define $\theta = 0$ to be the angle at which the brane embedding reaches its minimum value of y . From this expression, it is straightforward to check that for any value $y_0 > 1$,³ θ approaches a finite value as y goes to infinity, as indicated in figure 3.

Thus, the brane configurations asymptote to lines of constant θ .⁴ The relation between y_0 and the maximal value of θ is given by

$$\theta_\infty(y_0) = \int_{y_0}^{\infty} dy \frac{1}{y \sqrt{\frac{y_0^5(1+y^3)^{\frac{10}{3}}}{y_0^5(1+y^3)^{\frac{10}{3}}} - 1}} \quad (7)$$

³Recall that $y=1$ represents the IR end of the geometry.

⁴It is straightforward to check that configurations with $\theta = \text{const}$ are also solutions to the embedding equations. However, the brane cannot simply end at $y = 1$, so the only way to make such solutions (with fixed x_4 physical is to patch them on to another such solution which sits at the diametrically opposite point on the x_4 circle. This type of embedding and its generalizations were studied in the earlier work [13].

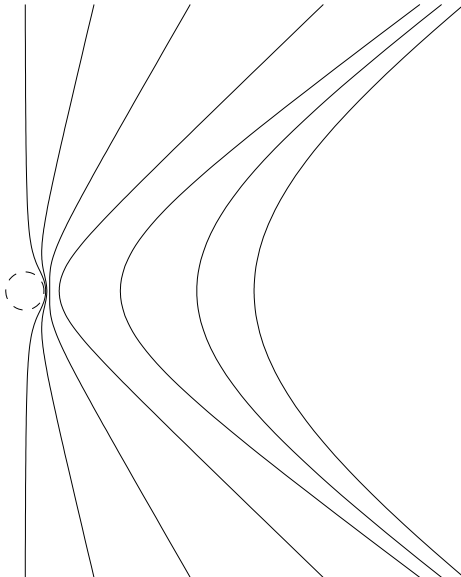


Figure 5: Examples of stable brane embeddings.

and plotted in figure 4. We see that for large y_0 , the asymptotic angle approaches the limiting value $\theta_\infty = \frac{\pi}{5}$. For $y_0 = y_*$, the two asymptotic ends of the brane go towards diametrically opposite points on the sphere. As y_0 approaches 1, θ_∞ increases without bound, corresponding to brane embeddings that wrap multiple times around the θ direction. Some representative embeddings are shown in figure 5.

As shown in figure 6, there exist discrete families of embeddings with the same asymptotics, which therefore correspond to different vacua in the same field theory. However, as we will see in the next section, all the embeddings with $\theta_\infty > \pi/2$ are unstable to “unwrapping,” i.e. slipping over the spherical hole in the geometry, as seen in figure 6. Thus, each field theory has at most one stable vacuum, and the stable theories are those with brane asymptotics $\theta_\infty \in (\frac{\pi}{5}, \frac{\pi}{2}]$. For the special case $\theta_\infty = \pi/2$ (corresponding to $y_0 = y_* = 1.0903795\dots$), the two ends of the probe brane go to diametrically opposite points on the S^5 . For these asymptotics, we actually have a family of embeddings related by the $SO(4)$ rotations that fix these diametrically opposite points on the sphere as shown in figure 7. This case corresponds to a spontaneous breaking of $SO(4) \rightarrow SO(3)$ (equivalently $SU(2) \times SU(2) \rightarrow SU(2)$), and we must therefore have an $SO(3)$ vector of massless goldstone bosons associated with the broken symmetry. It is these bosons that become tachyonic if increase θ_∞ beyond $\pi/2$ (or equivalently, try to decrease the minimum radial position y_0 below the value y_*). This is very similar to the naive brane picture in figure 1, where a tachyon develops if the transverse separation between the branes becomes too small.

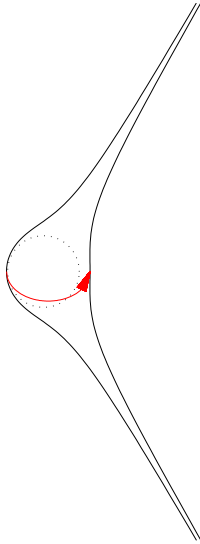


Figure 6: Example of multiple embeddings for the same brane asymptotics. There are additional embeddings with smaller y_0 and more “windings” around the sphere, however only the embedding with the largest y_0 is stable. The rest are perturbatively unstable to slipping around the sphere, as shown.

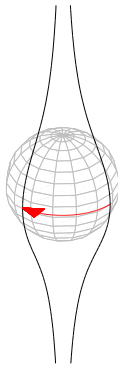


Figure 7: Geometrical interpretation of zero modes (massless mesons) for the special case $\theta_\infty = \pi/2$.

4 Meson spectrum and stability

In this section, we consider small fluctuations about the equilibrium brane configurations found in the previous section. We would like to determine which of the embeddings are perturbatively stable, and for these embeddings, to determine the spectrum of small fluctuations that gives the meson spectrum for the theory.

To determine the fluctuation spectrum, we start with the brane action (4) and expand to quadratic order about a chosen solution, parameterized by y_0 . We consider all possible bosonic fluctuations, which include fluctuations in the x_4 direction, fluctuations in the three transverse directions along the sphere (which we label by an $SO(3)$ triplet of scalar fields X_T), fluctuations in the $r - \theta$ plane, and the gauge field fluctuations.

In general, for the scalar field modes, the action for small fluctuations about the vacuum solution takes the form

$$S = -C \int d^4x \int_{y_0}^{\infty} dy \left\{ \frac{1}{2} A(y) \left(\frac{\partial \phi}{\partial x^\mu} \right)^2 + \frac{1}{2} \frac{\rho_0}{R^3} B(y) \left(\frac{\partial \phi}{\partial y} \right)^2 + \frac{1}{2} \frac{\rho_0}{R^3} C(y) \phi^2 \right\} \quad (8)$$

while for the gauge fields, we have

$$S = -C \int d^4x \int_{y_0}^{\infty} dy \left\{ \frac{1}{4} A(y) F_{\mu\nu} F^{\mu\nu} + \frac{1}{2} \frac{\rho_0}{R^3} B(y) F_{\mu y} F^{\mu y} \right\}$$

There are no mixing terms between gauge field and scalar fields at quadratic order.

For the various types of fluctuations, we find

Mode	$A(y)$	$B(y)$	$C(y)$
X_4	$\frac{(y^3-1)^2}{(y^3+1)^{\frac{1}{3}} y^{\frac{7}{2}}} R^{-1}(y)$	$\frac{(y^3-1)^2 (y^3+1)^{\frac{1}{3}}}{y^{\frac{5}{2}}} R(y)$	0
X_T	$\frac{(y^3+1)}{y^{\frac{9}{2}}} R^{-1}(y)$	$\frac{(y^3+1)^{\frac{5}{3}}}{y^{\frac{7}{2}}} R(y)$	$\frac{(y^3+1)^{\frac{5}{3}}}{y^{\frac{1}{2}}} \left(\frac{5y^3-1}{2y^3+1} - 1 \right) R^{-1}(y)$
θ	$\frac{(y^3+1)}{y^{\frac{5}{2}}} R(y)$	$\frac{(y^3+1)^{\frac{5}{3}}}{y^{\frac{3}{2}}} R^3(y)$	0
A_μ	$\frac{1}{y^{\frac{1}{2}} (1+y^3)^{\frac{1}{3}}} R^{-1}(y)$	$y^{\frac{1}{2}} (1+y^3)^{\frac{1}{3}} R(y)$	

where

$$R(y) = \sqrt{1 - \frac{y^5 (y_0^3 + 1)^{\frac{10}{3}}}{y_0^5 (y^3 + 1)^{\frac{10}{3}}}}.$$

4.1 Scalar fluctuations

The scalar fluctuation action above gives rise to an equation of motion

$$-A(y) \frac{\partial^2 \phi}{\partial x_\mu^2} - \frac{\rho_0}{R^3} \frac{\partial}{\partial y} \left(B(y) \frac{\partial \phi}{\partial y} \right) + \frac{\rho_0}{R^3} C(y) \phi = 0$$

We look for solutions of the form

$$\phi(x, y) = e^{ik \cdot x} f(y)$$

where $f(y)$ falls off fast enough so that the integral over y in the action converges (i.e. so that ϕ is a normalizable fluctuation). With this ansatz, the equation reduces to

$$-\frac{\rho_0}{R^3} \frac{\partial}{\partial y} \left(B(y) \frac{\partial f}{\partial y} \right) + \left(\frac{\rho_0}{R^3} C(y) - \lambda A(y) \right) f = 0$$

where $\lambda = m^2$ represents the four-dimensional mass of the fluctuation. The resulting Schrodinger-like equation can now be solved numerically to determine the values of λ for which normalizable solutions exist. These eigenfunctions are either even or odd functions in the θ coordinates.

We have used three different methods to determine the eigenvalues. The first is the “shooting method” in which the differential equation is numerically integrated starting from either even or odd boundary conditions at $y = y_0$. The parameter λ is then varied until the result drops to zero at large y .⁵

In the second method, we choose some complete basis of normalizable functions $h_n(y)$ (chosen to correspond to either even or odd boundary conditions at $\theta = 0$) and approximate

$$f(y) = \sum_{n=1}^N f_n h_n(y)$$

The action reduces to

$$S = \frac{1}{2} \sum_{m,n} f_m (\lambda A_{mn} + B_{mn} + C_{mn}) f_n$$

where

$$A_{mn} = \int dy A(y) h_m(y) h_n(y) \quad B_{mn} = \int dy B(y) h'_m(y) h'_n(y) \quad C_{mn} = \int dy C(y) h_m(y) h_n(y) .$$

The approximate eigenvalues are determined by extremizing the action, which gives the matrix eigenvalue equation

$$A^{-1}(B + C)f = \lambda f .$$

As we increase N , the eigenvalues determined in this way should converge to the exact ones (though the accuracy is much better for the eigenvalues λ_n with $n \ll N$).

In the third method, we determine the power series solutions of the differential equation about the points $y = y_0$ and $y = \infty$. We choose boundary conditions at $y = y_0$ corresponding to either an even or an odd function of θ , and boundary conditions at $y = \infty$ corresponding to a normalizable solution (the appropriate fall-off can be

⁵In practice, one looks for values of λ at which the solution switches from having positive values at large y to having negative values at large y or vice versa.

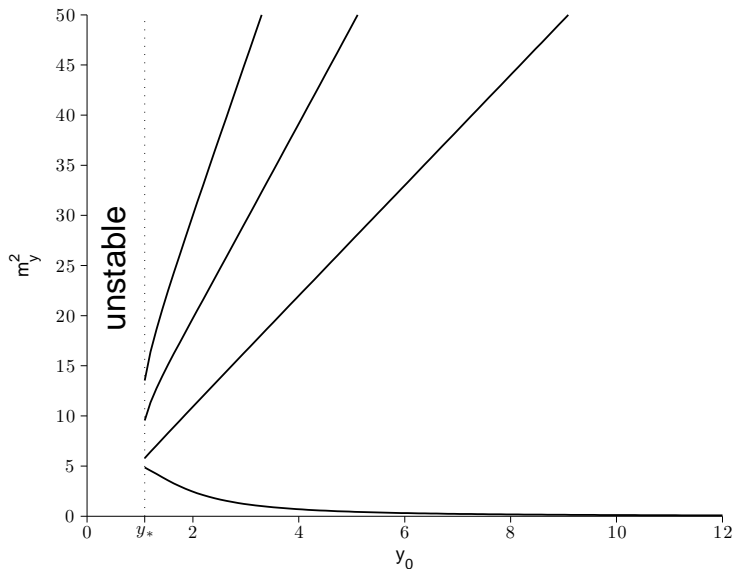


Figure 8: Spectrum of mesons arising from fluctuations of the brane embedding in the $y - \theta$ plane.

determined from the large y behavior of the differential equation). It can be shown that the large- y power series converges in the interval (y_0, ∞) , while the small y power series converges in the interval $[y_0, y_0 + \min(2y_0 - \frac{1}{y_0}, |y_0 - \frac{1}{2} - \frac{\sqrt{3}}{2}i|)]$. Thus, by choosing enough terms in each power series, there is a range of y values for which both series accurately approximate the corresponding exact solutions. Choosing one of these y values,⁶ we now search for values of λ for which the value and first derivative of the two power series can be made to match by a choice of normalization. For these values of λ the two power series can be patched together to give a good approximate solution, which is normalizable by construction.⁷ This method can be used to quickly generate very accurate results, except for values of y_0 close to 1, where the radius of convergence of the power series around y_0 is small, and an impractical number of terms in the large y power series is required to achieve accurate results.

Our results for the eigenvalues are summarized in figures 8,9,10, and 11, and the summary figure 2 in the Introduction. As we expected, we find that the lightest X_T fluctuation becomes massless at the value $y_0 \approx y_* = 1.0903795\dots$ This corresponds to $\theta_\infty = \frac{\pi}{2}$ where the two ends of the brane are diametrically opposite from each other and there is a family of embeddings with the same asymptotics related by $SO(4)$ transformations. The massless modes are goldstone bosons for the spontaneous breaking of $SO(4)$ (the symmetry preserved by the boundary conditions for the probe brane)

⁶In practice we choose a value for which addition an additional term to either power series gives the same fractional change in the function. At this point, the combined error from the two power series is minimized.

⁷Using Maple, we can calculate the power series coefficients analytically without approximation, so it is no problem to include 50 or more terms.

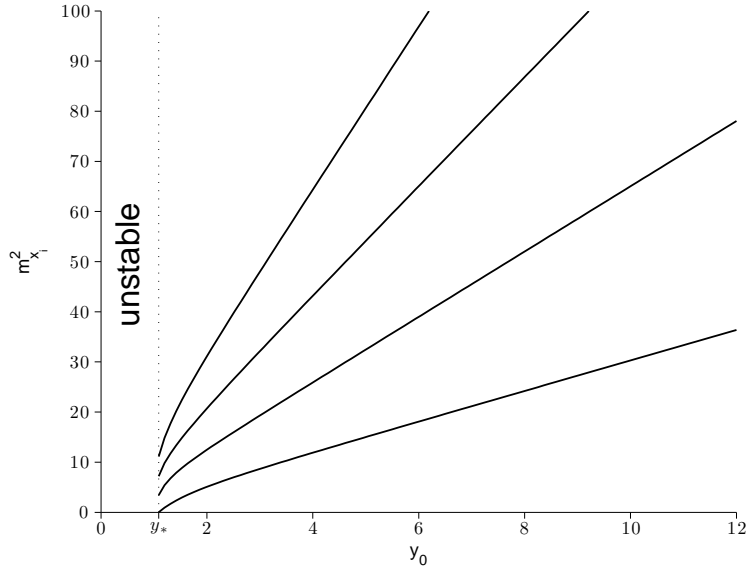


Figure 9: Spectrum of mesons arising from fluctuations of the brane embedding in the transverse sphere directions.

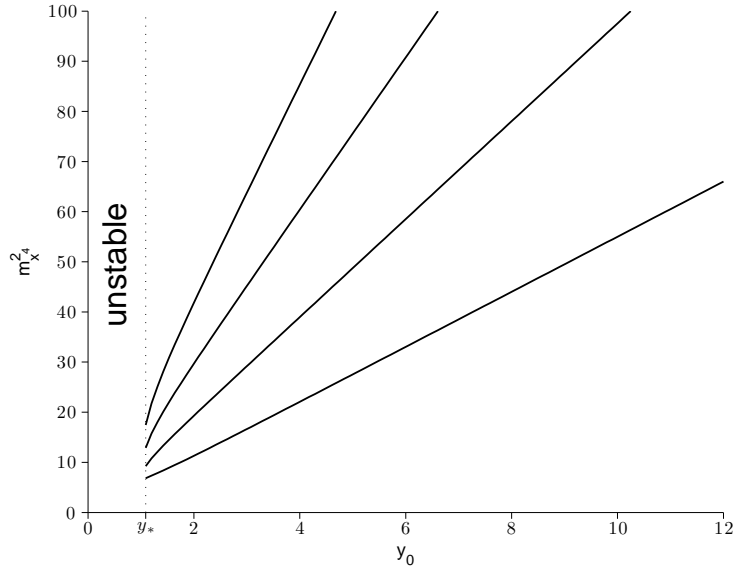


Figure 10: Spectrum of mesons arising from fluctuations of the brane embedding in the compact x_4 direction.

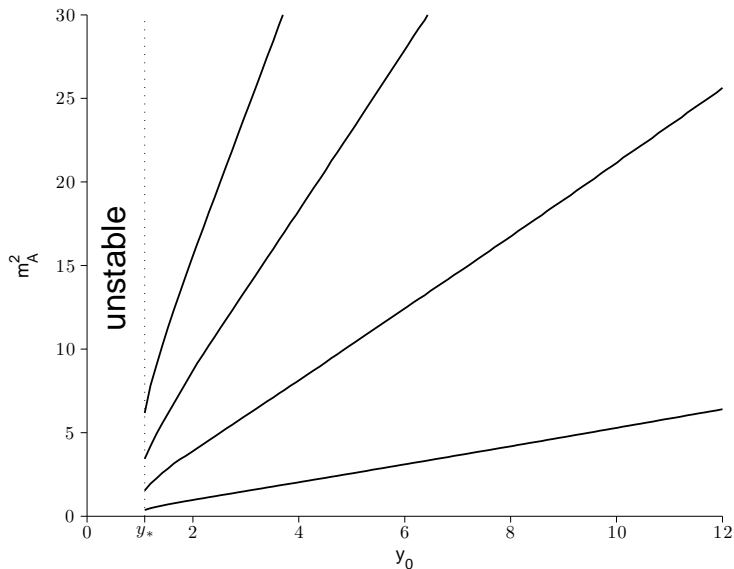


Figure 11: Spectrum of mesons arising from fluctuations of the gauge field on the probe D4-brane.

to $SO(3)$ (the symmetry preserved by the bulk embedding). For smaller values of y_0 , this mode becomes tachyonic, so the corresponding vacua in the field theory are perturbatively unstable.

For $y_0 > y_*$, we find that all fluctuations are massive. For almost all modes, we find that the large y_0 behavior of the mass goes like $m^2 \propto y_0$, consistent with an identification between y_0 and the bare quark mass in the field theory Lagrangian. However, strikingly, for one single scalar mode, the lightest fluctuation mode in the $r - \theta$ plane, we find a mass that goes to zero for large y_0 , $m^2 \propto y_0^{-2}$. One other notable feature of the spectrum for large y_0 is that the odd $r - \theta$ modes become degenerate with the even x_4 modes in the limit, as we can see in figure 2.

4.2 Interpretation of the light scalar

It is quite surprising that we should find a parametrically light scalar particle for large y_0 . In this limit, all the other meson states (and also the baryon states) become heavy, so the behavior is similar to a limit in QCD where the fundamental quark masses become large. If large y_0 corresponds to large quark mass in our case (as the naive brane configuration would also suggest), the lightness of our scalar mode must be due to a large binding energy for the quarks in this meson due to strong interactions. Typically, we would expect that such a parametric lightness would be associated with an approximate symmetry (e.g. the case of a pseudo-goldstone boson or broken SUSY). However, this is not quite true in our case.

From the bulk perspective, the crucial feature that leads to the appearance of this light mode is the fact that the brane asymptotics (i.e. the values of θ_∞) are very

similar for different large values of y_0 (recall that θ_∞ approaches a limit $\pi/5$ for large y_0). Thus, for large y_0 , we can get to a new extremum of the action with a very slight change in the asymptotics. In a sense, these different embeddings with nearby large values of y_0 are related by *almost-normalizable* fluctuations. If we did have normalizable fluctuations relating a continuous family of stable embeddings, these fluctuations would correspond to massless particles. So a way to understand why we have such a light mode is that we can get to another extremum of the action by a fluctuation which is almost normalizable. The actual light mode corresponds to a normalizable fluctuation that is very similar to this one (we have verified this explicitly).

Further insight into our light mode can be gained by noting that at large y_0 , the geometry is very similar to the supersymmetric near-horizon D4-brane geometry obtained by setting $f(U) = 1$ in (2). In this geometry, dual to D4-branes compactified with periodic boundary conditions for fermions, the probe brane action simplifies to

$$S = -\frac{\text{const}}{g_s} \int d\theta y^{\frac{3}{2}} \sqrt{y^2 + (y')^2} \quad (9)$$

It is straightforward to show that all solutions to the corresponding equations of motion have the form $y = y_0 f(\theta)$, where y diverges at the same asymptotic angle θ_∞ regardless of y_0 . The fluctuations that relate these solutions are normalizable, and correspond to an exactly massless scalar meson in the field theory. The situation is similar to that of [18], where a similar massless scalar could be understood as a Goldstone boson since the probe brane configuration spontaneously broke a conformal symmetry of the background geometry.⁸ However, in our case, the low-energy D4-brane theory is not conformally invariant, and the massless mode is not a Goldstone boson. The existence of a family of solutions with the same asymptotics in our case is related to the “generalized conformal symmetry” of the D4-brane background [19], in which a scaling of the radial coordinate y is combined with a change in the string coupling. Explicitly, we can see that the transformation

$$y \rightarrow \alpha y \quad g_s \rightarrow \alpha^{\frac{5}{2}} g_s$$

leaves the action (9) invariant. This is not a symmetry of the action, since we are changing the parameter g_s , but it does correspond to a symmetry of the classical equations of motion, which explains why there is a family of solutions related by the scaling $y \rightarrow \alpha y$. If we include g_s corrections (important when we go away from $N_c = \infty$), different terms in the quantum effective action will have different dependence on g_s , and so the scaling $y \rightarrow \alpha y$ will no longer be a symmetry of the (quantum corrected) equations of motion. To summarize, a modification of our field theory in which the adjoint sector is supersymmetric would have an exactly massless mode in the large N limit, but this is not a Goldstone boson since the associated “symmetry” involves changing a parameter of the theory (alternately, because the mode should receive a mass by quantum corrections when N is finite.) The light mode that we find for large

⁸We thank Ofer Aharony for pointing out this work, and providing the crucial insights that led to the interpretation in this paragraph.

y_0 arises because the geometry in our case is asymptotically the same as the geometry in the supersymmetric case.

Interestingly, the limit $y_0 \rightarrow \infty$ where our meson would become massless is the limit where the probe branes go off to radial infinity in the geometry. So despite having a mass that goes to zero, our light meson completely decouples from the adjoint degrees of freedom in this limit.

5 Baryons

By the gauge-theory / gravity dictionary, gauge fields in the bulk can be associated with conserved currents in the boundary theory. As in the Sakai-Sugimoto model, we have a gauge field living on the probe branes associated with our fundamental matter. This corresponds to the conserved baryon number (more precisely, quark number) current in the dual field theory. Specifically, the boundary value of the electrostatic potential A_0 (equivalently, the non-normalizable mode) corresponds to a chemical potential for baryon charge, while the electric flux at the boundary (equivalently, the normalizable mode of A_0) corresponds to the expectation value of baryon charge.

In order to have a state in the field theory with baryon charge, we need a source for electric flux on the probe brane. The simplest such source is a fundamental string endpoint (recall that the string action has a boundary term $\int A$ where A is the gauge field on the brane). We can think of such an endpoint as corresponding to a single fundamental quark. If a string has both of its ends on the probe brane, we have two endpoints, but with opposite orientations, so this corresponds to a mesonic state with a quark and anti-quark. In order to have a baryon state, we must have N_c strings with the same orientation ending on the probe brane. For a finite energy state, these strings must begin at some other source in the bulk. In our background, such a source is provided by D4-branes wrapped on S^4 [15]. These necessarily have N_c string endpoints, since the background D4-brane flux gives rise to N_c units of charge on the spherical D4-branes, so we need N_c units of the opposite charge (coming from the string endpoints) to satisfy the Gauss law constraint.

Thus, a finite energy configuration with a single unit of baryon charge is given by a D4-brane wrapped on S^4 together with N_c fundamental strings stretched between this D4-brane and the probe D4-branes. A special feature of our model is that these wrapped D4-branes can smoothly combine with the probe D4-brane (after shrinking the strings to zero size) to give a configuration with lower energy. In the final configuration, there are no explicit fundamental strings; we simply have a configuration of the probe brane that now wraps the S^4 . In the final configuration, the source for the electric field on the brane is the bulk flux of the Ramond-Ramond four-form, via the coupling $\int a \wedge F_4$.

Mathematically, the baryon charge in the field theory corresponds to an element of $\pi_4(S^4) = \mathbb{Z}$ associated with the embedding. To see this, note that the probe brane embeddings correspond to mappings to the bulk space from R^4 , topologically equivalent to a ball if we add the sphere at infinity. Given any probe brane embedding \mathcal{E} with the

same asymptotic behavior as the vacuum embedding \mathcal{E}_0 , we can define a map from a topological S^4 to the bulk spacetime by splitting the S^4 into two balls along an S^3 and using the maps \mathcal{E} and \mathcal{E}_0 to define the maps from the two balls. By considering only the sphere directions in the bulk, we can project this down to a mapping $S^4 \rightarrow S^4$, and such mappings may be associated with elements of the homotopy group $\pi_4(S^4) \sim \mathbb{Z}$. This integer gives the baryon number of the configuration in the field theory.

In order to find the actual bulk embedding corresponding to a single baryon, it is necessary to find the probe brane embedding with a single unit of winding on the S^4 (relative to the vacuum embedding) which has the minimum energy. Similarly, to find the bulk embedding corresponding to a nucleus with n baryons, we want to find the minimal energy brane embedding with n units of winding on the S^4 . In general, a numerical analysis will be required, but it should be possible to obtain precise results for the masses of small nuclei (certainly $n = 1$ and $n = 2$). Results for this will be presented in a follow-up paper.

6 Finite temperature

In this section, we will investigate the behavior of our model at finite temperature. In the $N_f \ll N_c$ limit that we are considering, thermodynamics is dominated by the adjoint sector of the theory. At a temperature $T_c = 1/(2\pi R)$, the model undergoes a deconfinement phase transition, in which the minimum action bulk solution changes from the original low-temperature solution to a black brane solutions with a horizon.

This transition is easy to understand in the Euclidean picture, where both the x_4 direction and the Euclidean time direction of the field theory are compactified with antiperiodic boundary conditions for the fermions. The lengths of the two compact directions are $2\pi R$ and $1/T$ respectively. For each value of T , we have two possible bulk solutions. The first is obtained from the Euclidean version of the zero temperature solution (1) simply by making an identification $\tau \sim \tau + 1/T$. The second is obtained by the replacements $2\pi R \leftrightarrow 1/T$ and $x_4 \leftrightarrow \tau$. In the first solution, the x_4 direction pinches off in the bulk geometry, while in the second solution, the τ direction pinches off in the bulk geometry (giving a horizon in the corresponding Minkowski solution). It turns out that the minimum action solution for a given R and T is the one where the smaller radius circle pinches off. Thus, the solution with a contractible time direction becomes dominant for $T > 1/(2\pi R)$.

For this high-temperature phase, the presence of a contractible time circle in the Euclidean solution means that the corresponding Minkowski solution is a black-brane solution with a horizon. The metric is given by

$$ds^2 = \left(\frac{U}{R_4}\right)^{\frac{3}{2}} (-f(U)dt^2 + \delta_{ij}dx^i dx^j + dx_4^2) + \left(\frac{R_4}{U}\right)^{\frac{3}{2}} \left(\frac{1}{f(U)}dU^2 + U^2 d\Omega_4^2\right) \quad (10)$$

where now

$$f(U) = 1 - \left(\frac{U_T}{U}\right)^3 \quad \frac{4\pi}{3} \left(\frac{R^3}{U_T}\right)^{\frac{1}{2}} = \frac{1}{T}$$

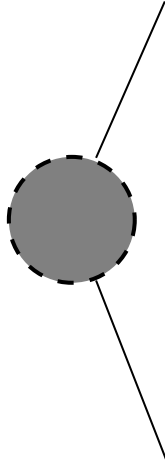


Figure 12: Schematic of “black hole” embeddings in which the brane extends down to the horizon.

As we did for the zero temperature case, we can now study the probe-brane action in this background and look for stable embeddings. Following the same steps, we find

$$S = -\mu_q \int d\sigma H(r) \sqrt{r^2 \left(\frac{d\theta}{d\sigma} \right)^2 + \left(\frac{dr}{d\sigma} \right)^2} \quad (11)$$

where

$$H_T(r) = \frac{r^{\frac{3}{2}}}{R^{\frac{3}{2}}} \left(1 + \frac{\rho_T^3}{r^3} \right)^{\frac{5}{3}} \frac{\left(\frac{r}{\rho_T} \right)^3 - 1}{\left(\frac{r}{\rho_T} \right)^3 + 1} \quad (12)$$

Now that we have a horizon, there are two qualitatively different types of embeddings for the D4-brane. Either the brane can remain entirely outside the black hole horizon (in what is known as a “Minkowski embedding”), or the brane can extend into the horizon (in a “black hole embedding”). In our model, the black hole embeddings are extremely simple, with each half of the brane sitting at some constant point on the S^4 , and extending in the radial direction from the horizon to $r = \infty$ as shown in figure 12. These embeddings exist for any value of the asymptotic angle. To see that these configurations are possible, we simply note that the equations of motion for the action (12) are satisfied if $\frac{d\theta}{d\sigma} = 0$.

To investigate solutions for which $\frac{d\theta}{d\sigma} \neq 0$, we can fix the reparametrization invariance by identifying $\sigma = \theta$. Defining also $y = r/\rho_T$, we get

$$S = -\frac{\mu_4}{g_s R^{\frac{3}{2}}} \rho_T^{\frac{5}{2}} \int d\theta h_T(y) \sqrt{y^2 + \left(\frac{dy}{d\theta} \right)^2}$$

where

$$h_T(y) = y^{-\frac{7}{2}} (1 + y^3)^{\frac{2}{3}} (y^3 - 1) .$$

Again, we can use the θ -independence of the action to deduce a conserved quantity

$$y' \frac{\partial S}{\partial y'} - S = \frac{h_T(y)y^2}{\sqrt{y^2 + (y')^2}}$$

The black-hole solutions above correspond to a value of 0 for this quantity (since $y' = \infty$ for those). For any nonzero value, the brane cannot reach the horizon, since $h_T(y) = 0$ at the horizon (where $y = 1$). Thus, all other embeddings are of the Minkowski type. For these, the brane reaches some minimal value $y = y_0$ where $y'=0$. We then have

$$\frac{h(y)y^2}{\sqrt{y^2 + (y')^2}} = h(y_0)y_0$$

which gives

$$\frac{dy}{d\theta} = \pm y \sqrt{\frac{h^2(y)y^2}{h^2(y_0)y_0^2} - 1}.$$

Integrating, we find

$$\theta(y) = \int_{y_0}^y \frac{dx}{x} \left(\frac{g(x)}{g(y_0)} - 1 \right). \quad (13)$$

where

$$g(x) = x^{-5}(x^3 - 1)^2(x^3 + 1)^{\frac{4}{3}}$$

and as before, we define $\theta = 0$ to be the angle at which the brane embedding reaches its minimum value of y .

The maximum value of θ for the embedding with minimum brane position y_0 is

$$\theta_\infty = \int_{y_0}^{\infty} \frac{dx}{x} \left(\frac{g(x)}{g(y_0)} - 1 \right). \quad (14)$$

This increases from $\theta_\infty = 0$ as y_0 approaches 1 to $\theta_\infty = \frac{\pi}{5}$ as y_0 goes to infinity. Thus, we find that Minkowski embeddings exist for precisely the theories where there is no stable vacuum. Furthermore, it is straightforward to verify that the black hole solution with the same asymptotic behavior always has a lower action. Hence, there is no regime of parameters for which the Minkowski embedding describes the equilibrium behavior of the field theory.

Summary

For the range of parameters where our holographic field theory has a stable vacuum solution at zero temperature, we have found that the only solution to the equations of motion for the probe brane in the high-temperature geometry is a black-hole embedding, where the two halves of the D4-brane extend directly into the horizon along the radial direction at constant position on the S^4 . Physically, the interpretation is that mesons “melt” as soon as the deconfinement transition is reached. This is in contrast to the Sakai-Sugimoto model and other models, where (for certain parameter choices)

there can be a window in temperature for which the theory is deconfined but there is still a well-defined meson spectrum.

One other consequence of our analysis is that for the special case where the two halves of the D4-brane come in from diametrically opposite points on the sphere, the full $SO(4)$ symmetry is restored in the high-temperature phase (recall that it was spontaneously broken to $SO(3)$ for low temperatures).

Acknowledgements

We would like to thank Andreas Karch, Moshe Rozali, Eric Zhitnitsky, and especially Ofer Aharony for helpful discussions and comments. This work has been supported in part by the Natural Sciences and Engineering Research Council of Canada, the Alfred P. Sloan Foundation, and the Canada Research Chairs programme.

A Alternate coordinates for θ fluctuations

In this appendix, we present the action for fluctuation of our probe D4-brane in the $y-\theta$ plane using an alternate parametrization that can be more convenient for numerical study. Parameterizing fluctuations in the embedding function $y(\theta)$ in terms of y as we have done above can be an inconvenient choice for a numerical analysis, since the “even” fluctuations result in a change of y_0 , and the choice of coordinates above essentially assumes that y_0 is fixed. A more straightforward choice is to take θ as the parameter.

The original action governing the embedding and the fluctuations in the r, θ directions is

$$S = -C \int d\theta H(y) \sqrt{y^2 + \left(\frac{dy}{d\theta}\right)^2 - f(y) \left(\frac{dy}{dt}\right)^2}$$

where

$$H(y) = y^{\frac{3}{2}} \left(1 + \frac{1}{y^3}\right)^{\frac{5}{3}}$$

and

$$f(y) = \frac{R^3}{\rho_0} y (1 + y^3)^{-\frac{2}{3}}.$$

Here, we have not included terms involving spatial derivatives in the field theory directions since these can be restored at the end by Lorentz invariance. Expanding about one of the solutions to the equations of motion, we get an action for small fluctuations given by

$$S = C \int d\theta \left\{ \frac{1}{2} A(y) (\partial_t \tilde{y})^2 - \frac{1}{2} B(y) (\partial_\theta \tilde{y})^2 - \frac{1}{2} C(y) \tilde{y}^2 - D(y) \tilde{y} \partial_\theta \tilde{y} \right\}.$$

We can integrate by parts and replace the last term with

$$\frac{1}{2} \tilde{y}^2 \partial_\theta D$$

Thus, it is equivalent to use an action

$$S = C \int d\theta \left\{ \frac{1}{2} A(y) \left(\frac{\partial \tilde{y}}{\partial x^\mu} \right)^2 - \frac{1}{2} B(y) \left(\frac{\partial \tilde{y}}{\partial \theta} \right)^2 - \frac{1}{2} C(y) \tilde{y}^2 \right\}$$

where A and B are as above and C is replaced by $C - \partial_\theta D$. Explicitly, we find that

$$\begin{aligned} A(y) &= \frac{Hf}{M^{\frac{1}{2}}} \\ B(y) &= \frac{Hy^2}{M^{\frac{3}{2}}} \\ C(y) &= \frac{\partial_y^2 H}{M^{1/2}} y^2 + \frac{\partial_y H}{M^{3/2}} (2y^3 - y^2 y'' + 4y(y')^2) + \frac{H}{M^{\frac{5}{2}}} (-2yy''(y')^2 + y^3 y'' + 2(y')^4 - y^2 (y')^2) \end{aligned}$$

where

$$M = y^2 + (y')^2$$

For numerical evaluation, it is convenient to use:

$$y' = \sqrt{\frac{H^2 y^4}{H_0^2 y_0^2} - y^2}$$

and

$$y'' = -y + \frac{HH'y^4}{H_0^2 y_0^2} + \frac{2H^2 y^3}{H_0^2 y_0^2}$$

The function y is determined implicitly in terms of θ by the equation

$$\theta(y) = \int_{y_0}^y dx \frac{1}{x \sqrt{\frac{H^2(x)x^2}{H^2(y_0)y_0^2} - 1}}$$

References

- [1] O. Aharony, S. S. Gubser, J. M. Maldacena, H. Ooguri and Y. Oz, “Large N field theories, string theory and gravity,” Phys. Rept. **323**, 183 (2000) [arXiv:hep-th/9905111].
- [2] E. Witten, “Anti-de Sitter space, thermal phase transition, and confinement in gauge theories,” Adv. Theor. Math. Phys. **2**, 505 (1998) [arXiv:hep-th/9803131].
- [3] A. Karch and E. Katz, “Adding flavor to AdS/CFT,” JHEP **0206**, 043 (2002) [arXiv:hep-th/0205236].
- [4] I. R. Klebanov and M. J. Strassler, “Supergravity and a confining gauge theory: Duality cascades and chiSB-resolution of naked singularities,” JHEP **0008**, 052 (2000) [arXiv:hep-th/0007191].

- [5] J. Babington, J. Erdmenger, N. J. Evans, Z. Guralnik and I. Kirsch, “Chiral symmetry breaking and pions in non-supersymmetric gauge / gravity duals,” *Phys. Rev. D* **69**, 066007 (2004) [arXiv:hep-th/0306018].
- [6] M. Kruczenski, D. Mateos, R. C. Myers and D. J. Winters, “Towards a holographic dual of large- $N(c)$ QCD,” *JHEP* **0405**, 041 (2004) [arXiv:hep-th/0311270].
- [7] T. Sakai and S. Sugimoto, “Low energy hadron physics in holographic QCD,” *Prog. Theor. Phys.* **113**, 843 (2005) [arXiv:hep-th/0412141].
- [8] S. A. Hartnoll, “Lectures on holographic methods for condensed matter physics,” *Class. Quant. Grav.* **26**, 224002 (2009) [arXiv:0903.3246 [hep-th]].
- [9] C. P. Herzog, “Lectures on Holographic Superfluidity and Superconductivity,” *J. Phys. A* **42**, 343001 (2009) [arXiv:0904.1975 [hep-th]].
- [10] P. Kovtun, D. T. Son and A. O. Starinets, “Viscosity in strongly interacting quantum field theories from black hole physics,” *Phys. Rev. Lett.* **94**, 111601 (2005) [arXiv:hep-th/0405231].
- [11] D. T. Son and A. O. Starinets, “Viscosity, Black Holes, and Quantum Field Theory,” arXiv:0704.0240 [hep-th].
- [12] S. S. Gubser and A. Karch, arXiv:0901.0935 [hep-th].
- [13] D. Gepner and S. S. Pal, arXiv:hep-th/0608229.
- [14] R. Casero, A. Paredes and J. Sonnenschein, “Fundamental matter, meson spectroscopy and non-critical string / gauge duality,” *JHEP* **0601**, 127 (2006) [arXiv:hep-th/0510110].
- [15] E. Witten, “Baryons and branes in anti de Sitter space,” *JHEP* **9807**, 006 (1998) [arXiv:hep-th/9805112].
- [16] H. Hata, T. Sakai, S. Sugimoto and S. Yamato, “Baryons from instantons in holographic QCD,” arXiv:hep-th/0701280.
D. K. Hong, M. Rho, H. U. Yee and P. Yi, “Dynamics of Baryons from String Theory and Vector Dominance,” arXiv:0705.2632 [hep-th].
D. K. Hong, M. Rho, H. U. Yee and P. Yi, “Chiral dynamics of baryons from string theory,” arXiv:hep-th/0701276.
K. Nawa, H. Suganuma and T. Kojo, “Brane-induced Skyrmions: Baryons in holographic QCD,” arXiv:hep-th/0701007.
K. Nawa, H. Suganuma and T. Kojo, “Baryons in Holographic QCD,” *Phys. Rev. D* **75**, 086003 (2007) [arXiv:hep-th/0612187].

- [17] O. Aharony, J. Sonnenschein and S. Yankielowicz, “A holographic model of deconfinement and chiral symmetry restoration,” *Annals Phys.* **322**, 1420 (2007) [arXiv:hep-th/0604161].
- [18] S. Kuperstein and J. Sonnenschein, “A New Holographic Model of Chiral Symmetry Breaking,” *JHEP* **0809**, 012 (2008) [arXiv:0807.2897 [hep-th]].
- [19] A. Jevicki, Y. Kazama and T. Yoneya, “Generalized conformal symmetry in D-brane matrix models,” *Phys. Rev. D* **59**, 066001 (1999) [arXiv:hep-th/9810146].
- [20] M. Van Raamsdonk and K. Whyte, in preparation